Dimensional Modification Induced Band Gap Tuning in 2D-Photonic Crystal for Advanced Communication and Other Application

R. R. Sathya Narayanan[1], T. Srinivasulu[1], Chitrank Kaul[1], Arvind Narendran[1], Ashit Sharma[1], Jhilick Ghosh[2], Nabanita Acharjee[2], and Kaustav Bhowmick[1(✉)]

[1] Photonics Research Lab, Department of Electronics and Communication Engineering, Amrita School of Engineering, Bengaluru, Amrita Vishwa Vidyapeetham, Amrita University, Bengaluru, India
k_bhowmick@blr.amrita.edu

[2] Netaji Subhash Engineering College, Kolkata, West Bengal, India

Abstract. We present a systematic simulation study of dimension-induced photonic band-gap tuning in two-dimensional (2-D), hexagonal lattice photonic crystals, consisting of air-holes in dielectric slabs. Photonic crystals are interesting candidates for application in various fields e.g. communication ranging from optical to THz regime, sensing, spectroscopy, imaging etc., using their property to trap and harness light and to produce high-Q resonances by the principle of localization and photonic bandgap formation. The insensitivity towards launched light wavelength shown herein by the bandgap response of a given 2-D planar photonic crystal is promising for enabling cheaper visible or NIR light sources to produce desired response in Mid-IR wavelengths with ease. The structures and material studied lie within the range of popular fabrication methodology. The results show that silicon photonic crystals, operated at 1.55 μm, can produce sharp resonances and large band transmission in Mid-IR wavelengths (3–5 μm) as well.

Keywords: Photonic crystal · Photonic band gap · Visible · NIR · MIR

1 Introduction

Interaction and manipulation of light and matter in photonic crystals (PhC) have mobilized the scientific community of photonics towards their exploration since their first appearance [1]. Despite an acquired understanding of the photonic bandgap (PBG) in such photonic structures [1, 2], further exploration of their optical properties continues [2]. The established wavelength-scalability in optical waveguides have been demonstrated in PhCs by Yablonovitch et al. [3], for a 3-D PhC in a microwave dielectric with refractive-index (r.i.) value similar to Si, to produce PBG-like forbidden bands in microwave ranges. Also, a Si 2.5-D PhC was shown [4] with PBG around 0.1 THz with 75 GHz ($\lambda \approx 3.99$ mm) to 110 GHz ($\lambda \approx 2.72$ mm) input.

Wavelength tuning and PBG tuning of various types have been reported for various application, e.g., Temperature-induced tuning of PBG-span [5] in 2012 and interlayers

N. Kumar and A. Thakre (Eds.): UBICNET 2017, LNICST 218, pp. 245–255, 2018.
https://doi.org/10.1007/978-3-319-73423-1_22

in the holes in 2.5-D PhCs shifting the band-edges of the minimum PBG 1.5–3% [6]. However, fabrication of such structures may be challenging in optical domain. In 1-D PhCs [1], varying N or number of layers and external stimulus like magnetic fields, can vary the PBG [7] although, refractive-index contrast between layers (Δn) remains a greater controlling factor [1]. Hence, availability of suitable material dictates the fabrication and usage. Other factors influencing the band-edge e.g. free-carrier injection around 1.9 μm [8], structural parameter tuning of band-gap in 2-D square lattice [9], effect on modal reflectivity of geometry tuning in photonic crystal [10], and, effect of various positions on grown oxide layer in Si on the band-gap [11] were also presented in the recent past.

Herein, we present a systematic simulation study of the effect of dimensional parameters in a hexagonal lattice 2-D PhC. As light red-shifts from visible to MIR, the cost of source laser increases manifold [12]. It is envisaged that using the dimensional band-gap tuning features in 2-D PhCs, a lower wavelength 1550 nm pulsed laser may be used to get desired operation in more expensive MIR ranges. Hexagonal lattice structures, which were found to be the best for fabrication of bent defects and better optical operation [1] were chosen. Analyses have been done based on two materials, namely, $Al_xGa_{1-x}As$ (x = 1) [13] for visible-to-NIR PBG shift study and Si [14–16] for NIR-to-MIR PBG shift study. The effective-indices for the PhC-structures were calculated using the effective-index method [17] and, the PBG features using plane-wave expansion method by MPB [1] and by FDTD-method using commercial software RSoft-FullWAVE [18]. The most important result hence found is a broadband response in MIR (3-5 μm) using Si PhC excited at 1550 nm laser pulse. Till date, applications based on Si for MIR are rare except for some studies on MIR high-Q resonance [19], using an expensive MIR tunable CW-laser at ~4.5 μm. The aforesaid result is important from the viewpoint of making 1550 nm communication devices using visible lasers and MIR (3–5 μm) spectroscopic devices on Si.

2 Simulation Work and Results

The material consideration, simulation work and Results with Discussion are presented in the following sub-sections.

2.1 Material Choice and Refractive-Index

The material(s) chosen for the present study were $Al_xGa_{(1-x)}As$ (x = 1) [13], for visible to NIR wavelengths, and Si [19] for NIR to MIR wavelengths. The principal criterion for the choices was to obtain a high enough absolute-index value at the chosen launch wavelength of the bulk absolute indices of $Al_xGa_{(1-x)}As$, the values for x = 1.0 (i.e., AlAs) are suitably high between λ = 650 to 700 nm in the visible range (with maximum current price of USD 702 [12]). The lower fractions of x provide high absolute indices, however, their UV-band-edges show successive red-shifts. Practically, AlAs being hygroscopic, it may need to be housed within some other material for usage. Similarly, data for Si absolute-index was obtained from three sources (for NIR excitation) [14–16]. Further, it was recognized that full 3-D FDTD simulation of PhC could be highly time-consuming with not

much of advantage [18]. Hence, the effective-index method [17] was adopted to find the effective-index of the PhCs. Figure 1 shows the schematic of a 2.5-D PhC and the direction of incident light along which the effective-indices were calculated for different 2.5-D PhCs studied, thus removing the slab- thickness and making 2-D simulation of the structure possible, for lower computational time. The correctness of the method was tested with that of a reported PhC structure [20] wherein the effective-index reported being ~2.797 at 1.55 μm.For the same work, we used the effective-index method and generated ~2.798 at 1.55 μm as the effective-index, which was close to the experimental measurement of refractive-indices. The convention shown for coordinate axes in Fig. 1(a), is at par with the convention used in the FDTD-solver of RSoft [18], and Fig. 1(b) shows the essential parameters of a 2.5D PhC.

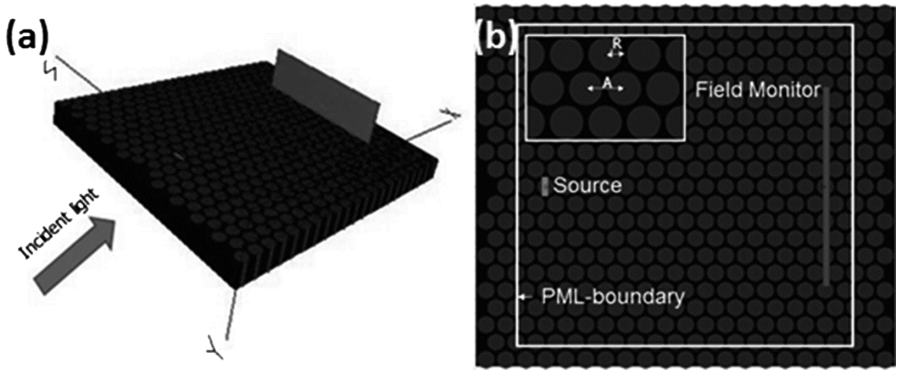

Fig. 1. (a) Schematic of typical 2.5-D PhC showing spatial coordinates used and light launching direction in which effective-index calculations have been performed. (b) A typical PhC (from Rsoft-FullWAVE) used in the present work showing the source, the field monitor and PML-boundary location. The inset shows the hole radius 'R' and period 'A'.

2.2 Numerical Verification of Simulation Mesh

Following the choice of materials and adopting the effective-index method, the simulation environment was setup using the ab-initio MPB software and the FDTD-based FullWAVE software. For both the cases first the verification of the mesh dependence of bandgap results were performed. For the said study, a 2.5-D PhC (shown in Fig. 1(b)) with hole-radii 'R' of 0.267 μm and period 'A' of 0.710 μm (both parameters as illustrated in Fig. 1(b) inset) were considered. The thickness of the 2.5-D structure was kept equal to the period 'A'. Maintaining the same structural parameters, different mesh size effects were studied in AlAs and in Si, with relevant effective-indices and launch-wavelengths (for FDTD). Invariably, throughout the present work, the launch light source have been considered to have a Gaussian distribution with the centre-wavelength as will be mentioned and with a 40 nm spread about the centre-wavelength, which is at the resolution limit of FullWAVE. Also, a PML [1] boundary was chosen and was position-optimized in the order of $\lambda/2$ near the source and the monitor, both of which are shown in Fig. 1(b).

A schematic of the PML boundary is shown in Fig. 1(b), drawn along the true simulation boundary, to make the location visible. Actual PML thickness is chosen as per optimization of the output till the achievement of mesh-independence. TE-mode excitation was done in each case. The band-gaps in the same structure were found using MPB, and was studied for different grid-sizes (which in MPB is in terms of number of k- points [1]), namely, 4, 25, 81, 100, in succession, chosen for random increase of fine-ness. The two cases studied had effective-indices ~3.018 at 700 nm (Al-As) and ~3.343 at 1532 nm (Si). However, the band gap obtained (in MPB) had very low percentage variation (order of $10^{-3\%}$), with mean-square error calculated as $\sqrt{\left(PBG\_mesh_{j-1} - PBG\_mesh_j\right)^2 / \left(PBG\_mesh_j\right)^2}$, with no appreciable pattern.

However, in the case of FullWAVE, some appreciable mesh-to-mesh errors were obtained, using the same error formula, which is shown for AlAs and Si, in Fig. 2. The RSoft mesh study was done with grid-sizes 0.071 μm, 0.0473 μm, 0.035 μm and 0.01 μm, in the order of increasing fine-ness, in two ways, namely, error % between each progressively finer mesh-pair, and, error % between the coarsest mesh 1 paired with progressively finer meshes. The mesh error analyses shows that other than the coarsest first mesh in FDTD, the finer meshes quickly fall below 5% error which is statistically acceptable. Also, a plateau-ing trend can be observed, which is confirmed by Fig. 2(b), depicting increasing error with the coarsest mesh 1. Hence, the fineness of meshes 2 to 4 were maintained, as appropriate for the subsequent simulations. All dimensions have been chosen bearing the minimum dimension that can be fabricated by e-beam lithography, i.e. 0.2 μm.

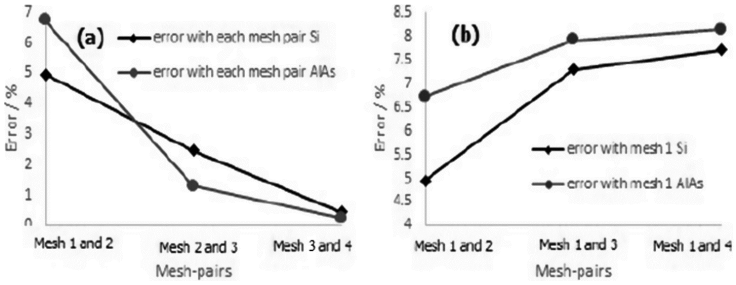

Fig. 2. Mesh error analyses: (a) error between mesh pairs, coarse to fine; (b) error between coarsest mesh 1 paired with each progressively finer mesh, in terms of PBG.

2.3 Simulation of Al-As PhC

For the Al-As PhC mentioned in Sect. 2.2, the results of PBG-analyses are presented here. The result of MPB simulation is presented in Fig. 3(a), with the corresponding band-edges in wavelength marked as (a) 1724 nm and (b) 2573 nm (see the gray band). Only the TE-like PBG was sought and not the complete band-gap [1]. Similarly, using FDTD solver, the same structure was simulated with Gaussian light centered at 680 nm (Fig. 3(b)) effective-index ~3.030, and at 700 nm (Fig. 3(c)) with effective-index ~3.018. In the FDTD results, the y-axis depicts transmitted modal intensity arbitrary units (a.u)

and the PBG is where the transmission is at zero-level. In both the cases, it can be seen that the band-gap and band-edges are approximately constant and in agreement with the MPB solution showing that visible light in a suitable PhC can produce PBG in NIR to MIR region. Similar studies were carried out for different R/A ratios and the trend curve is presented in Sect. 2.5.

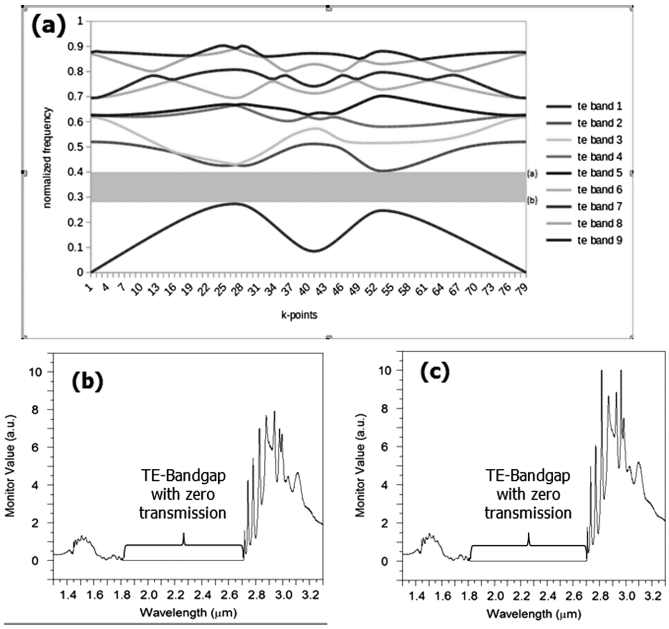

Fig. 3. Al-As PhC simulation for R = 0.267 μm, A = 0.71 μm excited in TE-mode; (a) MPB results showing PBG between as 1724 nm and 2573 nm; (b) FDTD simulation for 680 nm showing similar PBG as in (a); (c) FDTD simulation for 700 nm showing similar PBG as in (a).

2.4 Simulation of Si PhC

Following the PBG obtained from NIR to MIR in Al-As PhC, it was tested whether the established Si technology could produce PBG deeper into the MIR, to cover the 3–5 μm region, where the absorptive losses are the least. Thus, a PhC with the same R/A ratio was considered but, made in Si, with an effective-index ~3.343 at 1532 nm. The results of the same are presented as simulated in MPB (Fig. 4(a)) and FDTD (Fig. 4(b)). It can be seen that the PBG obtained in the present case extends from ~2.0 μm to 3.0 μm in the MIR. The results for various values of R/A are presented in Sect. 2.5.

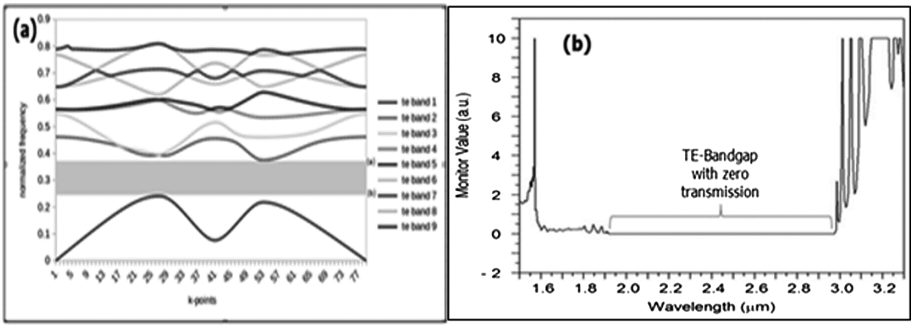

Fig. 4. Si PhC simulation for R = 0.267 μm, A = 0.71 μm excited in TE-mode; (a) MPB results showing PBG between as 1900 nm and 2900 nm (gray shaded band); (b) FDTD simulation for 1532 nm showing similar PBG as in (a).

2.5 Trend Curves in PBG and R/A Ratio

As mentioned in Sects. 2.3 and 2.4, the exercises were repeated for different values of R/A for both Al-As and Si PhCs, the trends of which are shown here. The R/A ratio has been identified in the theory of PhCs as the major structural parameter [1]. So, for the present study, certain major variations of the ratio were identified and the corresponding variations of the PBG were recorded. The choice of values for R and A was based on obtaining the maximum PBG and the input lights were taken as 850 nm for Al-As and 1532 nm for Si, with appropriately calculated effective-indices. Firstly, the value of

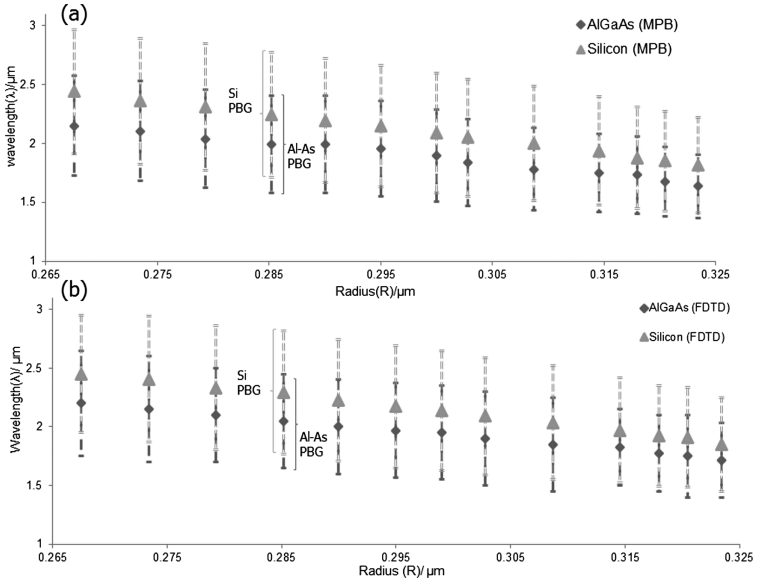

Fig. 5. Hole radius 'R' variation at period 'A' = 0.71 μm: (a) MPB; (b) FDTD.

period 'A' was fixed at 0.71 μm, and the hole-radius 'R' was increased. The result for the same is shown in Fig. 5(a) and (b) for MPB and FDTD, respectively. Figure 5 is oriented such that each data point shows the center-wavelength of PBG for either Al-As or Si, with the error-bars depicting the PBG span on either side of the centre-wavelength. Both simulation tools show that by increasing 'R' for a given 'A' the center-wavelengths of the PBGs show a blue-shift, accompanied by a simultaneous slight and progressive decrease in the PBG-span.

Thereafter, the hole-radius 'R' was fixed at 0.3 μm and increasing the period 'A'. The input lights were chosen same as in the previous. The results of the study show a trend opposite to that of varying 'R' with a fixed 'A' (see Fig. 6). The MPB and FDTD results are again found to have a good agreement (Fig. 6(a) and (b), respectively).

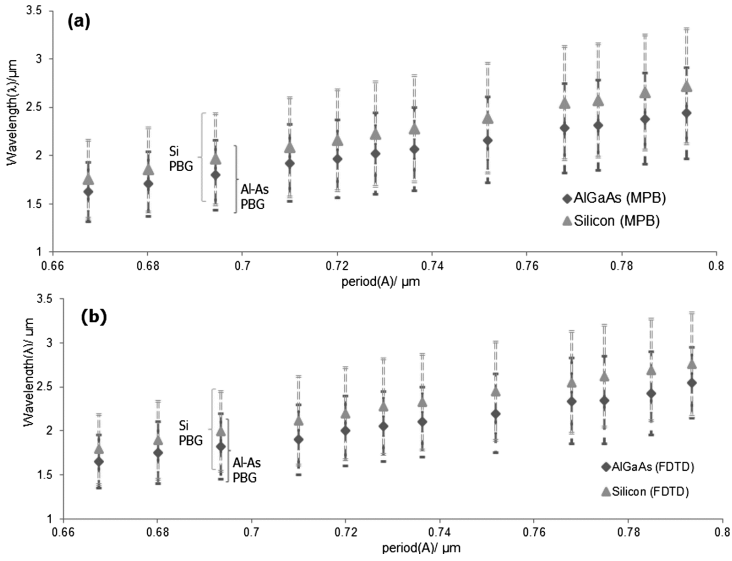

Fig. 6. Period'A' variation at hole radius 'R' = 0.3 μm simulated by: (a) MPB; (b) FDTD.

Finally, R/A ratio was taken with R = 0.3 μm and A = 0.65 μm, wherein 'R' and 'A' were simultaneously increased and decreased by factors representing ±2.4%, ±5% etc. The results of study are presented in Fig. 7. Again, Fig. 8(a) shows the results from MPB, while Fig. 7(b) shows the results from FDTD. While the R/A is always maintained, the PBG spread can be seen to remain more or less the same, with little variation. However, the simultaneous decrease in R and A shows a blue-shift in the center-wavelength of PBG and a simultaneous increase in R and A shows a red-shift.

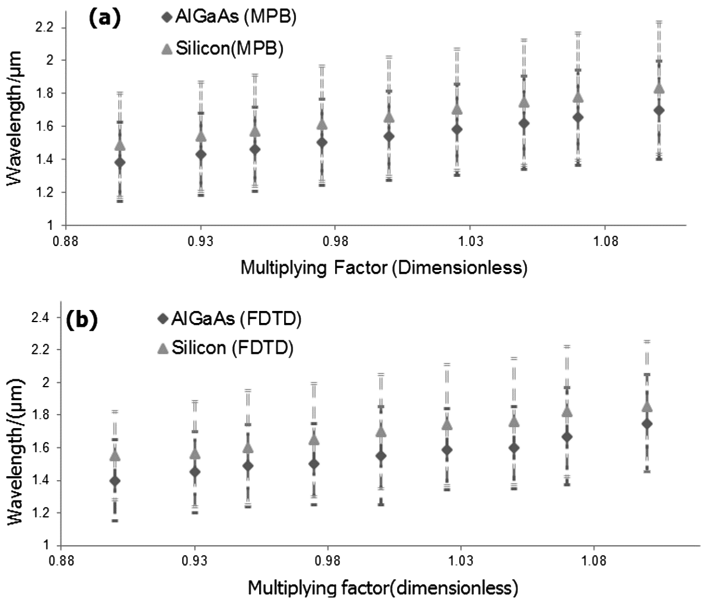

Fig. 7. Effect of period 'A' and hole-radius 'R' simultaneously varying by percentages, keeping the R/A ratio constant, about the central values of R = 0.3 μm and A = 0.65 μm.

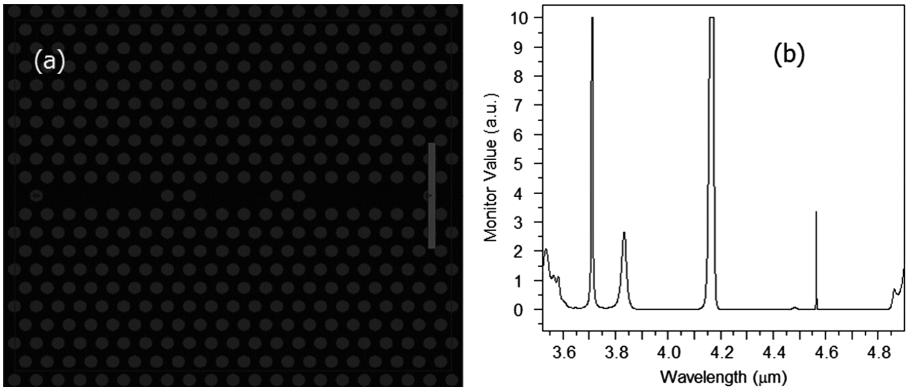

Fig. 8. Si MIR operation study: (a) Line defect(s) in Si 2-D photonic crystal at 1532 nm light source; (b) high intensity resonant peak and narrow high intensity band in 3–5 μm MIR range.

Overall, the study presented in Sect. 2.5 shows that by the interplay of dimensional parameters 'R' and 'A' with chosen wavelength, hence, refractive-index of the structure at the chosen wavelength, the PBG can either be blue-shifted or red-shifted. As can be seen from Figs. 5, 6 and 7, even a visible transparent material like Al-As can be illuminated with suitable coherent light, and the PBG may be obtained in MIR. The same can be achieved with the Si-technology. Thus, cheaper material and laser options may be utilized to obtain PBG in MIR and THz, where optical-sources and transparent material

are otherwise expensive, and may help to develop long-wavelength devices, using defect light-localization [1], as discussed in Sect. 3.

3 Suggestive Devices Possible for MIR

Some preliminary MIR devices were simulated based on the concept presented in Sect. 2. Figure 8(a) shows a Si Photonic crystal with R = 0.304 μm and A = 1.012 μm, ordained by a series of line-defects created, which was simulated by FDTD with an input light of 1532 nm. It can be seen that a sharp high intensity resonant peak and a narrow, high intensity band is obtained in the 3-5 μm band (see Fig. 8(b)). The peaks are similar to resonant peaks possible to obtain with defect modes in PhC [1], but in the low-absorption MIR-band with light source at 1532 nm. Potential application of such spectral response lies in the resonance dependent application [20], but at a cheaper cost of material and source.

Further, a waveguide without any discontinuity can be formed in the same PhC, as shown in Fig. 9(a). It can be seen that a high-intensity band is obtained, between 3.6 μm to 4.8 μm wavelengths (see Fig. 9(b)), which can be used for spectroscopic application, for which 3–5 μm wavelength region is mostly sought. Further study maybe performed on the same for sensing and free-space communication.

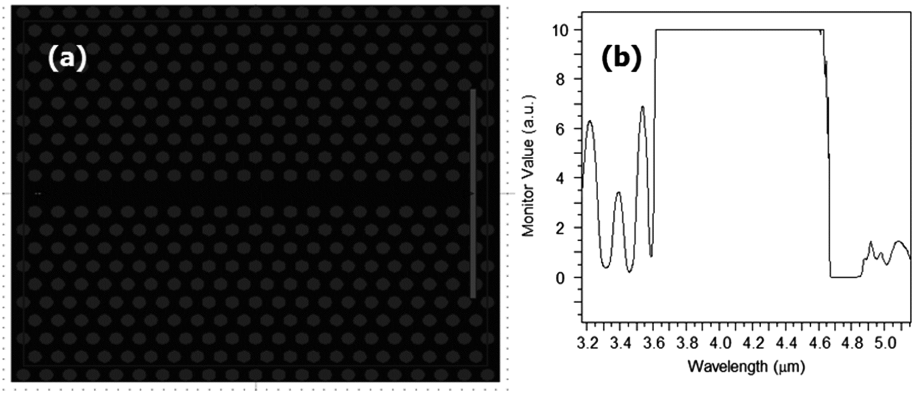

Fig. 9. Si MIR broadband operation study: (a) Waveguide line defect in Si 2-D photonic crystal at 1532 nm light source; (b) high intensity broadband response in 3–5 μm MIR range.

A final study was done in the present work, to find out how the aforesaid wavelength band between 3.6 μm to 4.8 μm might change with varying thickness of the PhC slab, which in effect would vary the effective-index of the slab. The result of the same is presented in Fig. 10(a). It can be seen within the range of thicknesses studied, the band remains unchanged, demonstrating a high stability over thickness. However, with higher thickness, slightly lower intensity was obtained as shown in Fig. 10(b), compared to that shown in Fig. 9(b).

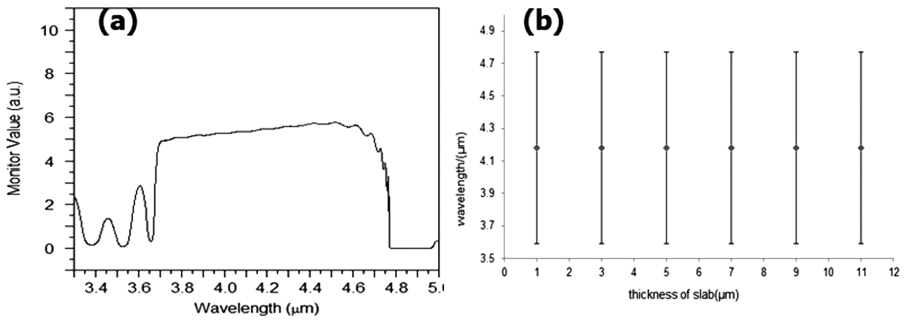

Fig. 10. Si MIR broadband operation study: (a) High intensity broadband response in 3–5 μm MIR range for 2-D PhC shown in Fig. 10 (thickness = period), but with thickness 11 μm, showing lower yet high, intensity; (b) unchanged bandwidth in 3–5 μm with increasing thickness.

Thus, with all the studies presented in the current work, the structural parameters 'R' and 'A' play the most important part in the optical outputs from the structures. Following the parameters mentioned, wavelength of source has some effect on the span of the PBG. However, the effect of the thickness is largely nil as it is compensated by the effective refractive-index at a given wavelength.

4 Conclusion

A detailed study of the effect of structural parameters of 2-D hexagonal-lattice photonic crystals (PhC) have been presented. The study brings out the fact that in 2-D PhCs, the hole-radii and period between holes are the most important parameters controlling the spectral response of such crystals, which have been hinted earlier. The new fact that came to light from the present work is that it is possible to manipulate the span and location of the photonic band-gap to a great extent. Such tuning capability have been presented as capable of producing long wavelength devices for communication and many other application, using 2-D PhCs made of cheaper material, using cheaper and shorter wavelength sources. The resulting trends show the promise of developing cheap broadband MIR devices as well for spectroscopy and free-space communication, which will be further explored in our future works.

References

1. Joannopoulos, J.D., Johnson, S.G., Winn, J.N., Meade, R.D.: Photonic Crystals: Molding the Flow of Light, 2nd edn. Princeton University Press, Princeton (2008)
2. Kitzerow, H.: Tunable photonic crystals. Liq. Cryst. Today **11**(4), 3–7 (2002)
3. Yablonovitch, E., Gmitter, T.J., Leung, K.M.: Photonic band structure: the face-centered-cubic case employing nonspherical atoms. Phys. Rev. Lett. **67**(17), 2295–2298 (1991)
4. Kim, J.I., Jeon, S.G., Kim, G.J., et al.: Two-dimensional terahertz photonic crystals fabricated by wet chemical etching of silicon. J. Infrared Milli Terahz Waves **33**, 206–211 (2012)

5. Suthar, B., Kumar, V., Kumar, A., Singh, K., Bhargava, A.: Thermal expansion of photonic band gap for one dimensional photonic crystal. Prog. Electromagnet. Res. Lett. **32**, 81–90 (2012)
6. Glushko, A., Karachevtseva, L.: PBG properties of three-component 2D photonic crystals. In: International Conference on Photonics and Nanostructures - Fundamentals and Applications, vol. 4, no. 3, November 2008
7. Chun-Zhen, F., Jun-Qiao, W., Jin-Na, H., Pei, D., Er-Jun, L.: Theoretical study on the photonic band gap in one-dimensional photonic crystals with graded multilayer structure. Chin. Phys. B **22**(7), 074211-1–074211-5 (2013)
8. Leonard, S.W., van Driel, H.M., Schilling, J., Wehrspohn, R.B.: Ultrafast band-edge tuning of a two-dimensional silicon photonic crystal via free-carrier injection. Phy. Rev. B **66**, 161102-1–161102-4 (2002)
9. Muhammad, H.M., Jamil, N.Y., Abdullah, A.I.: Photonic bandgap tuning of photonic crystals by air filling fraction. Raf. J. Sci. **24**(5), 96–102 (2013)
10. Sauvan, C., Lecamp, G., Lalanne, P., Hugonin, J.P.: Modal-reflectivity enhancement by geometry tuning in photonic crystal microcavities. Opt. Exp. **13**(1), 245–255 (2005)
11. Thitsa, M., Albin, S.: Band gap tuning of macro-porous si photonic crystals by thermally grown SiO2 interfacial layer. ECS Trans. **11**(17), 1–9 (2008)
12. [online resource]. www.thorlabs.com. Accessed 30 Mar 2017
13. Pikhtin, A.N., Yaskov, A.D.: Sov. Phys. Semicond. **14**(4), 389–392 (1980)
14. Aspnes, D.E., Theeten, J.B.: Spectroscopic analysis of the interface between si and its thermally grown oxide. J. Electrochem. Soc. **127**(6), 1359–1365 (1980)
15. Frey, B.J., Leviton, D.B., Madison, T.J.: Temperature dependent refractive index of silicon and germanium. In: International Conference on Proceedings of SPIE 6273 (Orlando) (2007)
16. Green, M.A., Keevers, M.J.: Optical properties of intrinsic silicon at 300 K. Prog. Photovoltaics Res. Appl. **3**, 189–192 (1995)
17. Coldren, L.A., Corzine, S.W., Masanovic, M.L.: Introduction to optical waveguiding in simple double-heterostructures. In: Diode Lasers and Photonic integrated circuits, 2nd edn., New Jersey, Ap. 3, sec. 3, pp. 551–554 (2012)
18. [online resource]. https://optics.synopsys.com/rsoft/rsoft-passive-device-FullWAVE.html. Accessed 30 Mar 2017
19. Shankar, R.: Mid-infrared photonics in silicon. Ph.D. thesis, Harvard University, April 2013
20. Lee, C., Thillaigovindan, J.: Optical nanomechanical sensor using a silicon photonic crystal cantilever embedded with a nanocavity resonator. Appl. Opt. **48**(10), 1797–1803 (2009)